JOURNAL OF MATERIALS SCIENCE 23 (1988) 3939–3944

Fracture toughness of silicon nitride determined by cyclic-fatigue-cracked specimens

Y. MUTOH, K. TANAKA, T. NIWA, N. MIYAHARA
Department of Mechanical Engineering, Technological University of Nagaoka, Nagaoka-shi 940-21, Japan

An experimental technique for determining fracture toughness has been developed. In this method, a fatigue precrack is introduced in single-edge notched beam specimens by cyclic fatiguing in four-point bend at an elevated temperature. The resulting fatigue precracks satisfy all conditions required by the ASTM Standard Test for plane-strain fracture toughness of metallic materials. The applicability of this technique to provide reproducible fracture toughness values is demonstrated by experimental results obtained for silicon nitride sintered in two different ways in comparison with those obtained by means of the indentation technique for the same materials.

1. Introduction

The method of the determination of the plane-strain fracture toughness K_{IC} was already established and standardized for metallic materials, e.g. ASTM E339 [1]. However, up to now, there seems no generally accepted method of K_{IC} determination for ceramics, although various types of specimens and testing methods have been attempted [2]. Some typical examples of fracture toughness test practised are the single-edge notched beam method [3, 4], the chevron notched method [5, 6], the controlled surface flaw method [7, 8], the indentation technique [9, 10], the bridge compression method [11, 12] and the cyclic compression method [13]. A major problem in the K_{IC} determination is the precracking and notch preparation. The effect of notch width or notch radius is very sensitive to K_{IC} in such brittle materials as ceramics [3, 14]. From this respect, the bridge compression method and the cyclic compression method are promising, since these methods can introduce an "ideal" precrack. However, these relatively new methods have not yet been investigated thoroughly and cannot avoid some limitations. In the bridge compression method, a rectangular bar specimen made a hardness indentation on the top surface is supported on an anvil and compressed with two rectangular punches, one on each side of the indentation. The artifacts of the geometrical and load variables affect so sensitively the morphology of the bridge compression cracks that there is a difficulty in the reproduction of precracks with a same size. In the cyclic compression method, a fatigue precrack is introduced in single-edge-notched specimens loaded in uniaxial cyclic compression, the local zone of damage during cyclic compression is fully embedded in material elastically strained in far-field compression. Thus, the length of the precrack is limited to the length of the local damage zone at the notch root, i.e. the notch root radius. In view of the limitations associated with the various fracture testing methods currently available for brittle solids, a continuing research effort requires new test procedures to be established.

It has been represented here that precracks can be introduced into silicon nitride single-edge-notched beam (SENB) specimens by cyclic fatiguing at an elevated temperature. This procedure can provide accurate fracture toughness values satisfying the ASTM Standard Test Method for the plane-strain fracture toughness of metallic materials.

TABLE I Additives and densities of silicon nitrides

	Additives (wt %)			ϱ_{th}	ϱ	ϱ_r
	Y_2O_3	Al_2O_3	AlN	($Mg\,m^{-3}$)	($Mg\,m^{-3}$)	(%)
S-Si_3N_4	6.2	1.4	–	3.26	2.85	87.5
HIP-Si_3N_4	8.0	–	4.0	3.27	3.27	100

ϱ_{th} theoretical density, ϱ density, ϱ_r relative density.

2. Experimental procedures

2.1. Materials and specimens

Two silicon nitrides were examined. HIP-Si_3N_4 was supplied for the main tests and S-Si_3N_4 for the preliminary tests. The amount of additives and the relative density for each material are listed in Table I, and Young's modulus and Vickers hardness in Table II. HIP-Si_3N_4 is pressurelessly pre-sintered at 2073 K and sintered at 1973 K to almost 100 per cent density by a hot isostatic press. S-Si_3N_4 is pressurelessly sintered at 2073 K, both have β-crystalline structure. Both the bending strength and SENB specimens of the two silicon nitrides were cut from billets using a diamond saw. The specimen dimensions differed between the materials and testing procedures as shown in Table III.

TABLE II Young's modulus E and Vickers hardnesses H_v of silicon nitrides

	E (GPa)	H_v (GPa)
S-Si_3N_4	204	6.56
HIP-Si_3N_4	320	15.67

0022–2461/88 $03.00 + .12

TABLE III Specimen dimensions

	Kind of bend test	B	W	a_0	L	l
S-Si_3N_4	Fatigue precracking : 4-point	5	4	1	40	20
	Fracture toughness : 3-point	5	4	1	27	–
HIP-Si_3N_4	Bending strength : 3-point	4	3	–	27	–
	Fatigue precracking : 4-point	4.85	10	4	40	20
	Fracture toughness : 3-point	4.85	10	4	40	–

Those dimensions indicated were the thickness B, width W, support span length L and loading span length l. Both sides of all the specimens were surface-ground along the length of the specimens with a 600 grit diamond wheel; the maximum surface roughnesses of which were less than 0.5 μm. SENB specimens were notched at the centre by a diamond wheel to a depth of $a = 4.0$ mm for HIP-Si_3N_4 specimen and $a = 1.0$ mm for S-Si_3N_4, with the notch width $N = 0.3$ mm and the notch radius $r = 0.15$ mm. After the notch was machined, the thickness sides in the vicinity of the notch were polished with a diamond paste in order to make the observation of the fatigue cracks easier.

2.2. Bending strength test

Bending strength tests were conducted in a vacuum (4×10^{-5} torr) by three-point bending, using six different temperatures between room temperature (RT) and 1673 K. They were carried out under a loading rate of 0.5 mm min^{-1} using an Instron-type tensile testing machine, and the peak load to failure, P_f, was noted.

2.3. Fatigue precracking and fracture toughness tests

Precracking by fatigue was carried out in air at 1473 K using a servohydraulic testing machine. This was done for a four-point bend under a load control of the stress ratio $R\ (= P_{min}/P_{max}) = 0.1$ at 1 Hz. Fig. 1 shows the results of the fatigue fracture tests of SENB specimens for HIP-Si_3N_4 plotted as the relationship between net section stress amplitude and the number of cycles to failure. With reference to the SN curve, the stress amplitude of 65 MPa was adopted as the standard loading level to introduce a fatigue precrack. The precracking was performed by the following two methods in order to examine the effect of the maximum stress intensity factor at the fatigue precracking, K_{fmax}, on the fracture toughness K_c. One method is the constant amplitude loading method (Method I) as illustrated in Fig. 2a; After the initial 8000-cycle block test at constant stress amplitude of 65 MPa (the apparent maximum stress intensity factor K_{fmax} will correspond to 6.5–7.0 MPa$^{1/2}$, if the length of the possible fatigue crack is not included and the notch length is assumed to be equal to that of crack) the test was interrupted to observe the fatigue crack. When the length of the fatigue crack reached 0.4–0.5 mm the test was stopped. The test was continued until the appearance of the relevant length of crack, interrupting the test every 4000 cycles to measure the crack length. The other method is the K_{fmax} decreasing method (Method II) as illustrated in Fig. 2b; the stress amplitudes were decreased following the sequence of blocks from 65 MPa to 40 MPa and then interrupted to observe the fatigue crack. When the length of the crack attained 0.4–0.5 mm, the test was stopped. When the crack length was not attained the test was continued at the stress amplitude of 40 MPa until the appearance of the relevant length of crack as periodically interrupted to measure the crack length.

The terminal values of K_{fmax} for these two methods were evaluated at almost 7.7 MPa m$^{1/2}$ and 4.4 MPa m$^{1/2}$, respectively. Here, the length of the precrack plus that of the notch was equalized to the length of crack and the evaluation was done according to the formulation obtained from a handbook edited by Tada *et al.* [15]. Fracture toughness tests were carried out on the precracked specimens at various temperatures from RT to 1473 K in the same way as the bending strength test.

In comparison with the SENB fracture toughness test, the indentation technique was also performed. On all the SENB specimens tested, Vickers diamond pyramid indentations were made by using loads 49–490 N with hold times 10–30 sec. In each specimen, three points for the same loading condition were

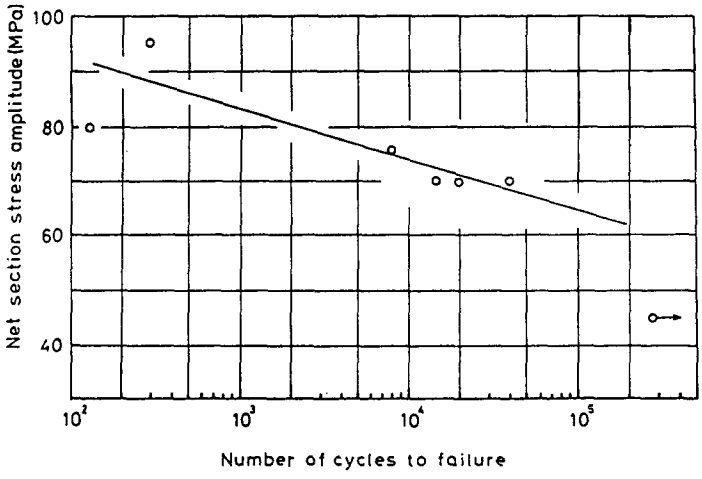

Figure 1 S-N curve at 1473 K for HIP-Si_3N_4 SENB specimen. $R = 0.1$.

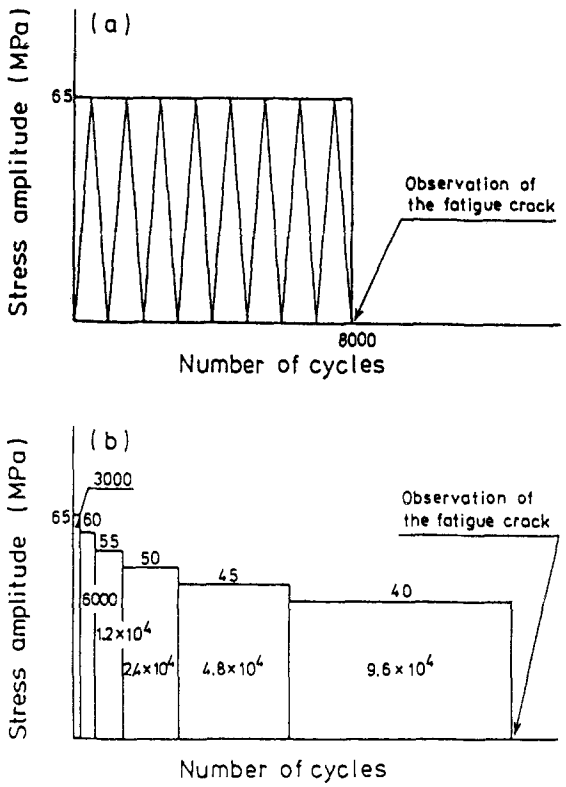

Figure 2 The sequence of block loading for precracking. (a) The constant K_{fmax} method. (b) The decreasing K_{fmax} method.

indented and their median cracks were carefully measured by means of an optical microscope. The indentation fracture toughness was evaluated according to the following formulation [16],

$$K_c = 0.0725P/a^{3/2}.$$

3. Experimental results

3.1. Bending strength

Fig. 3 shows the results of the bending strength test for HIP-Si_3N_4. The strength σ_B was calculated from the conventional elastic formulation, $\sigma_B = 3P_fL/2BW^2$. The strength at room temperature was about 920 MPa. With the increase in temperature, the strength showed a gradual reduction up to 1173 K, but above the temperature, the reduction rate increased rapidly.

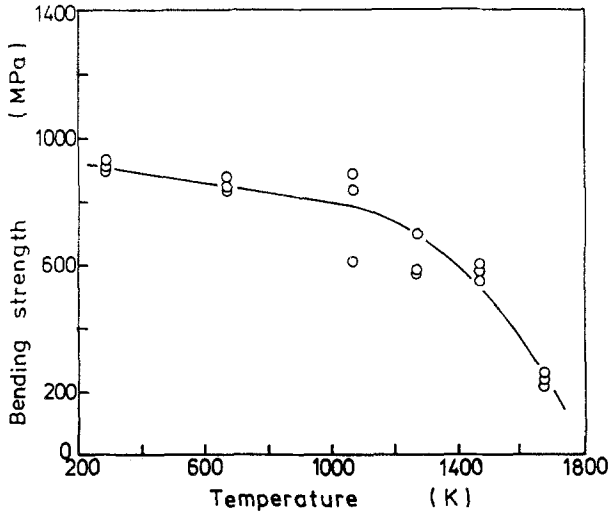

Figure 3 Relationship between bending strength and temperature for HIP-Si_3N_4.

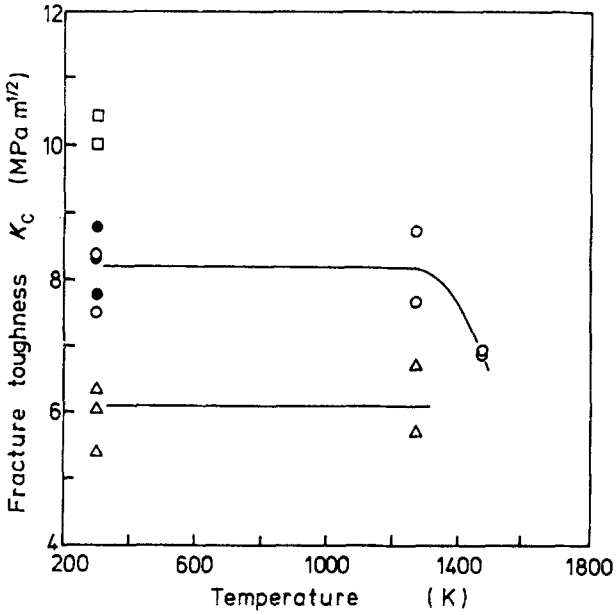

Figure 4 Relationship between fracture toughness and temperature for HIP-Si_3N_4. ○ K_{fmax} = 4.4 MPa m$^{1/2}$, ● K_{fmax} = 7.7 MPa m$^{1/2}$, □ notched (R = 0.15). For S-Si_3N_4 △ K_{fmax} = 2.8 MPa m$^{1/2}$.

3.2. Fracture toughness test for fatigue precracked specimens

Fig. 4 represents the relationship between fracture toughness and temperature. Values of fracture toughness K_c appeared to be almost independent of temperature up to 1273 K for both the materials, but decreased slightly at 1473 K for HIP-Si_3N_4. The relevant values were around 8 MPa m$^{1/2}$ at the lower temperatures and 7 MPa m$^{1/2}$ for HIP-Si_3N_4, and 6 MPa m$^{1/2}$ at the lower temperatures for S-Si_3N_4. Fig. 4 indicates that no significant difference in K_c values can be found between the high K_{fmax} (= 7.7 MPa m$^{1/2}$) test and the low K_{fmax} (= 4.4 MPa m$^{1/2}$) test, although the latter satisfies the condition, $K_{fmax} \leqslant 0.6K_{IC}$, while the former does not. This fact suggests that the ASTM Standard condition can be mitigated for ceramic materials. The figure also exhibits the results for notched specimens with root radius r = 0.15 mm. These were much higher than those for precracked specimens. The fact, of course, emphasizes the effectiveness of the fatigue precracking.

Fig. 5 shows an optical micrograph of the fatigue crack at the notch root observed on the specimen surface of an HIP-Si_3N_4. An example of the fatigue crack front resulting from such an experiment is illustrated in Fig. 6. These figures indicate that the fatigue

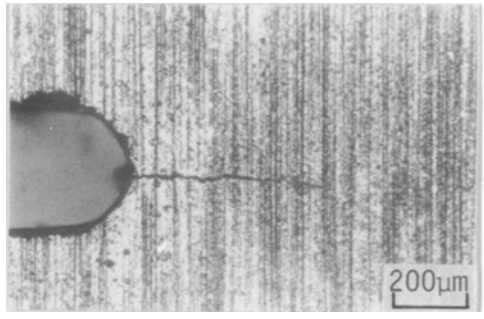

Figure 5 An optical micrograph of a fatigue crack at a notch root in HIP-Si_3N_4.

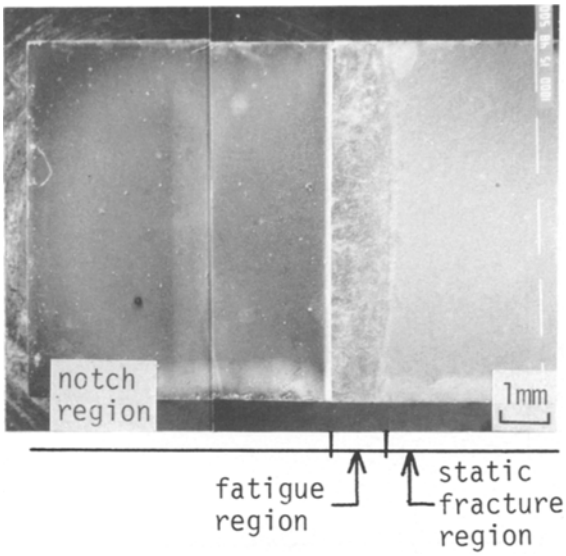

Figure 6 An SEM micrograph of a fracture surface in HIP-Si_3N_4.

crack appeared as sharp and as straight as that in metallic materials, and that the crack front was straight through and unambiguously determinable. Fig. 7 demonstrates the detailed view of the fracture surface. The fatigue crack surface looked glassy and was distinguishable from the static fracture surface. There was no difference in these observations between HIP-Si_3N_4 and S–Si_3N_4 specimens. Fig. 8 shows a result of X-ray microanalysis on such a fracture surface in S-Si_3N_4 specimen. This indicates that nitrogen was replaced by oxygen on the fatigue fracture surface. Hence it was evident that the glassy surface was formed by abrasion and oxidation attack during fatigue crack propagation.

3.3. Indentation fracture toughness

Fig. 9 indicates the relationships between the indentation crack length a and the applied load P for the two materials. These were correlated, on average, with the P–$a^{3/2}$ relations as the two respective full lines. The relevant K_c values were 7.3 MPa $m^{1/2}$ for HIP-Si_3N_4 and 5.2 MPa $m^{1/2}$ for S-Si_3N_4. For comparison, the fracture toughness values obtained by using fatigue precracked specimens are also evaluated as P–$a^{3/2}$ relationships and the results were shown in the figure by the respective two broken lines for the two materials. The latter values were positioned in the side of slightly larger magnitude for each material compared with the average indentation toughness relation, but almost of the same magnitude compared with the upper bound of the data scatter in the indentation fracture toughness.

4. Discussions

4.1. Validity as a plane strain fracture toughness test

It is obvious from Fig. 5 that the lengths of the fatigue precrack introduced satisfied the following requirement of ASTM E399: the length of the fatigue crack on each surface of the specimen shall not be less than 2.5% of W (= 0.25 mm for HIP- and 0.10 mm for S-Si_3N_4 specimens). It is also clear from Fig. 6 that the following requirements applied to the fatigue crack front were satisfied: (1) The difference between any two of the three crack length measurements shall not exceed 10% of the average crack length. (2) The surface crack length measurements shall not differ from the average crack length by more than 15%, and the differences between these two measurements shall not exceed 10% of the average crack length.

Furthermore, it is required in the standard for valid K_{IC} that both the specimen thickness B and the crack length a exceed $2.5(K_{IC}/\sigma_{ys})^2$, where σ_{ys} is the 0.2% offset yield strength. In general, the yield strengths of such brittle materials as ceramics cannot be determined, and thus the fracture strengths for smooth specimens may be used instead. In the present study, the fracture strengths were obtained only for HIP-Si_3N_4 and so the following discussion will refer to this material. The yield strengths to satisfy the requirement shall exceed 190 MPa at RT and 1273 K, and 166 MPa at 1473 K. These are much lower than the fracture strengths of 920 MPa at RT, 620 MPa at 1273 K and 580 MPa at 1473 K, respectively.

4.2. Effect of fatigue damage on fracture toughness

In the cycling test at 1473 K, the plastic deformation or intergranular sliding at the crack tip causes the fatigue crack formation. The plastic strain induced at the crack tips may remain as residual stress and affect the fracture toughness at lower temperatures. If this is very influential, the fracture toughness at RT will be dependent on the value of K_{fmax} applied at 1473 K. However, the results in Fig. 4 did not vary with K_{fmax}. This indicates that, in the present study, the residual

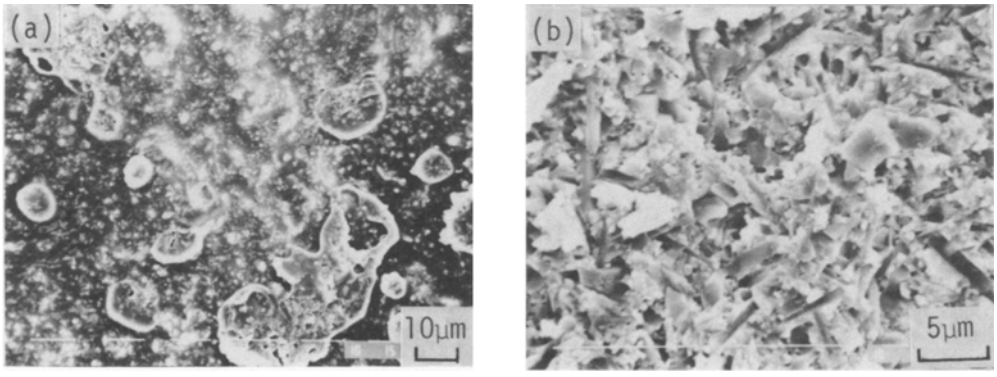

Figure 7 SEM fractographs for a HIP-Si_3N_4 fracture toughness specimen. (a) Fatigue fracture region. (b) Static fracture region.

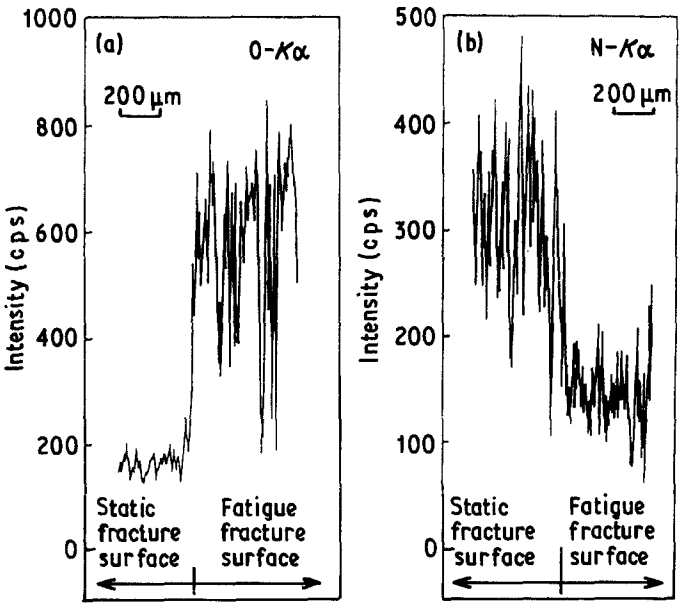

Figure 8 X-ray microanalysis on the fracture surface for S-Si_3N_4 specimen. (a) Oxygen profile. (b) Nitrogen profile.

stress at the crack tip did not affect the fracture toughness, but, generally speaking, the K_{fmax} decreasing method is more desirable to avoid the possible effect of residual stress.

Fig. 7 shows the occurrence of oxidation on the fatigue fracture surface. The resulting oxide film may influence the fracture toughness. If the oxide film is assumed to consist of SiO_2, silicon nitride can be oxidized according to the following reaction

$$Si_3N_4 + 3O_2 \rightarrow 3SiO_2 + 2N_2.$$

Since the specific weights are 3.18 Mg m^{-3} for Si_3N_4 and 2.22 Mg m^{-3} for SiO_2 and the atomic weights are 140.3 g for Si_3N_4 and 44.1 g for SiO_2; it is anticipated from the reaction that the volume of Si_3N_4 surface film expands 1.84 times by the oxidation. The expansion causes the crack closure at the crack tip during the fracture toughness test at low temperatures. This may explain the reason for the slightly higher values in fatigue precracking fracture toughness than those in indentation fracture toughness.

4. Conclusions

An experimental technique for determining fracture toughness in ceramics has been developed. In this method, a fatigue precrack is introduced in SENB specimens by cyclic fatiguing in a four-point bend at an elevated temperature. The fatigue precracks formed in the present study satisfy all the conditions required by the ASTM Standard Test Method for plane-strain fracture toughness of metallic materials (E399). Subsequently the valid fracture toughness values can be obtained by using the fatigue precracked specimens.

From the results of fracture toughness tests on two kinds of silicon nitride at the temperatures between room temperature and 1473 K, the fracture toughness values were almost constant below 1273 K but decreased above 1273 K. The values at room temperature were almost equal to, or rather higher than, those obtained by the indentation technique. The slightly higher values are attributed to the occurrence of crack closure resulting from the formation of oxide film on the fatigue fracture surface.

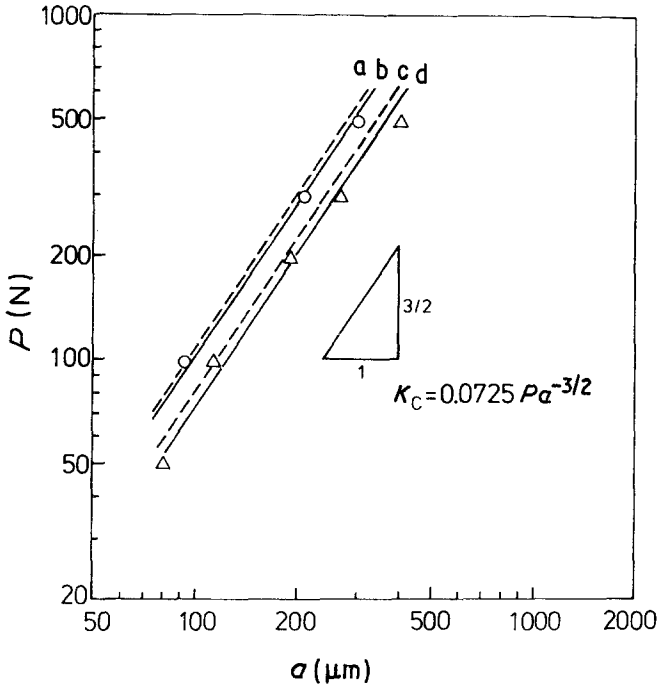

Figure 9 Relationship between indentation crack length and applied load. ○ HIP-Si_3N_4, △ S-Si_3N_4, --- fatigue precracked SENB. a K_c = 8 MPa m$^{1/2}$, b K_c = 7.3 MPa m$^{1/2}$, c K_c = 6 MPa m$^{1/2}$, d K_c = 5.2 MPa m$^{1/2}$.

Acknowledgements

This work was supported by a Grant-in-Aid for Science Research (No. 60550048) from the Ministry of Education, Science and Culture, Japan. The authors are also indebted to Shin-Etsu Chemical Co., Ltd., and Toshiba Tangaloy Co., Ltd. for preparing the specimens.

References

1. ASTM E399, Standard Test Method for Plane-Strain Fracture Toughness of Metallic Materials.
2. A. G. EVANS, "Fracture Mechanics of Ceramics", Vol. 1, edited by R. C. Bradt, C. P. H. Hasselman and F. F. Lange (Plenum, New York, 1974) p. 17.
3. R. L. BERTOLOTTI, *J. Amer. Ceram. Soc.* **56** (1973) 107.
4. R. KNEHAUS and R. STEINBRECH, *J. Mater. Sci. Lett.* **1** (1982) 327.
5. L. M. BARKER, *Engng Fract. Mech.* **9** (1977) 361.
6. D. MUNZ, R. T. BUBSEY and J. E. SRAWLEY, *Int. J. Fract.* **16** (1980) 359.
7. J. J. PETROVIC, L. A. JACOBSEN, P. K. TALTY and A. K. VASUDEREVAN, *J. Amer. Ceram. Soc.* **58** (1976) 113.
8. J. J. PETROVIC, *J. Amer. Ceram. Soc.* **66** (1983) 277.
9. B. R. LAWN and T. R. WILSHAW, *J. Mater. Sci.* **10** (1975) 1049.
10. A. G. EVANS and T. R. WILSHAW, *Acta Metall.* **24** (1976) 939.
11. T. SADAHIRO and S. TAKATSU, *Modern Dev. Powder Metall.* **14** (1980) 561.
12. T. NOSE and T. FUJII, *J. Amer. Ceram. Soc.* **71** (1988) 328.
13. S. SURESH, L. EWART, M. MADEN, W. S. SLAUGHTER, M. NGUYEN, *J. Mater. Sci.* **22** (1987) 1271.
14. I. TAKAHASHI *et al., J. Ceram. Soc. Japan* **93** (1985) 186.
15. H. TADA, P. C. PARIS and G. R. IRWIN, "The stress analysis of cracks handbook" (Del Research Corp., 1973).
16. K. TANAKA, *J. Jpn Inst. Metals* (in Japanese) **48** (1984) 1157.

Received 27 July
and accepted 23 October 1987